



Synthesis :: Materials :: Corrosion :: Environment :: Energy

YuCorr

Analyse :: Discover :: Coat :: Green :: Protect :: Save :: Sustain

INTERNATIONAL CONFERENCE
MEĐUNARODNA KONFERENCIJA

MEETING POINT OF THE SCIENCE AND PRACTICE IN THE FIELDS OF
CORROSION, MATERIALS AND ENVIRONMENTAL PROTECTION

*STECIŠTE NAUKE I PRAKSE U OBLASTIMA KOROZIJE,
ZAŠTITE MATERIJALA I ŽIVOTNE SREDINE*

PROCEEDINGS

KNJIGA RADOVA

Under the auspices of the
MINISTRY OF EDUCATION, SCIENCE AND TECHNOLOGICAL
DEVELOPMENT OF THE REPUBLIC OF SERBIA

Pod pokroviteljstvom
MINISTARSTVO PROSVETE, NAUKE I TEHNOLOŠKOG RAZVOJA
REPUBLIKE SRBIJE

May 16-19, 2022 :: Divčibare, Serbia

**XXIII YUCORR IS ORGANIZED BY
*ORGANIZATORI XXIII YUCORR-a***



SERBIAN SOCIETY OF CORROSION AND MATERIALS PROTECTION

Udruženje Inženjera Srbije za Koroziju i Zaštitu Materijala



**INSTITUTE OF CHEMISTRY, TECHNOLOGY AND METALLURGY,
UNIVERSITY OF BELGRADE**

*Institut za Hemiju, Tehnologiju i Metalurgiju,
Univerzitet u Beogradu*



UNION OF ENGINEERS AND TECHNICIANS OF SERBIA, BELGRADE

Savez Inženjera i Tehničara Srbije



ENGINEERING ACADEMY OF SERBIA

Inženjerska Akademija Srbije

Hardness and morphology analysis of electrolytically produced copper coatings

Analiza tvrdoće i morfologije elektrolitički dobijenih bakarnih prevlaka

Ivana O. Mladenović^{1,*}, Nebojša D. Nikolić¹

¹ University of Belgrade, Institute of Chemistry, Technology and Metallurgy, Njegoševa 12, 11 000 Belgrade, Serbia

*I.O.M. Email: ivana@nanosys.ihm.bg.ac.rs

Abstract

The influence of various electrolysis parameters, such as selected operating current regime, the cathode material type, composition and mixing conditions of the electrolyte and electrodeposition time, on the structural-morphological characteristics of the copper coatings has been investigated. Morphology and structure of the coatings were analyzed by scanning electron microscope (SEM) and atomic force microscope (AFM). Characterization of mechanical performance, such as microhardness of the coating, was done using the Vickers microindentation test. The absolute hardness of Cu coatings was determined by application of the composite hardness models, named the Chicot–Lesage (C–L). Based on this model, it is determined the critical relative indentation depth (RID)_c of 0.14, independent of all examined parameters of the electrodeposition. Depending on the electrolyte type, two different Cu coatings were obtained: fine-grained microcrystalline coatings with a strong (220) preferred orientation from the basic sulfate electrolyte and smooth mirror bright nanocrystalline coatings with a strong (200) preferred orientation from the electrolyte with added leveling/brightening additives. The „softening effect“ of mirror bright coatings obtained in the presence of a combination of additives is explained by the grain boundary phenomenon. Two different substrates: monocrystalline silicon Si(111) and polycrystalline brass alloy, were selected for comparative analysis of composite hardness.

Keywords: *electrodeposition; Vickers microhardness; copper coating; composite hardness model*

Izvod

Istražen je uticaj različitih parametara elektrolize, kao što je izbor radnog režima struje, katodnog materijala, sastav i uslovi mešanja elektrolita i vreme taloženja, na strukturno-morfološke karakteristike bakarnih prevlaka. Analizirana je morfologija i struktura prevlaka pomoću skenirajućeg elektronskog mikroskopa (SEM) i mikroskopa na principu atomskih sila (AFM). Karakterizacija mehaničkih performansi, kao što je mikrotvrdoća prevlaka, urađena je korišćenjem mikro utiskivača po Vickersovom testu. Apsolutna tvrdoća bakarnih prevlaka je određena primenom modela kompozitne tvrdoće, pod nazivom Šiko–Lezaž (Š–L). Na osnovu ovog modela određena je kritična relativna dubina utiskivanja (RDU) od 0,14 koja je bila nezavisna od svih ispitivanih parametara elektrohemijskog taloženja. U zavisnosti od tipa elektrolita, dobijene su dve različite prevlake bakra: sitnozrna mikrokristalna prevlaka bakra iz osnovnog sulfatnog elektrolita sa izraženom (220) preferencijalnom orijentacijom i glatka ogledalasto sjajna nanokristalna prevlaka bakra sa izraženom (200) preferencijalnom orijentacijom iz elektrolita sa dodatkom aditiva za poravnanje/sjaj. „Efekat omekšavanja“ ogledalasto sjajnih prevlaka dobijenih u prisustvu kombinacije aditiva je objašnjen preko fenomena uticaja granice zrna. Za uporednu analizu tvrdoće kompozita odabrana su dva različita supstrata: monokristalni silicijum Si(111) i polikristalna legura mesinga.

Ključne reči: *elektrohemijsko taloženje; Vickersova mikrotvrdoća; bakarna prevlaka; kompozit; model tvrdoće*

Introduction

Nanostructured materials, such as thin metallic coatings or laminates, whose thickness does not exceed 10 μm , have become attractive for use in microelectromechanical system (MEMS) industries due to their specific structural, chemical and mechanical properties in relation to the bulk form of the same material [1]. In its monocrystalline form, copper may be considered as a soft material with a small ability to resist deformations that is, it has low microhardness. For example, the bulk form of polycrystalline copper substrate has a hardness of 0.37 GPa [2]. Conventional polycrystalline Cu coatings electrodeposited galvanostatically from basic sulfate electrolyte has a grain size in the micron range or a grain size in the nano range electrodeposited from electrolyte with added leveling/brightening additives [3].

Indentation testing is reliable test method for the evaluation of mechanical properties of bulk, thin-coating materials and laminate structure of different materials over a wide range of size scales [4, 5]. In the case of thin coatings deposited on the substrate, the dominant effect of the coating hardness is only if the contact surface is small. The response of the system to the indentation is called "composite hardness" and it depends on coating thickness and microstructural and mechanical properties of the coating and the substrate, together. In addition to the dimension of the contact surface, both materials show a number of phenomenological effects during indentation, known in the literature and described as "Indentation Size Effect", ISE effect [6-8]. In order to determine an absolute hardness of the coating, it is necessary to apply composite hardness models or use very low indentation loads. There are a number of mathematical models that adequately describe the mechanical response of a composite system during microindentation and used for estimation absolute hardness of coating, such as the Chicot-Lesage [9-12], Korsunsky [13], Chen-Gao [14], Burnett-Rickerby (B-R) [15], etc.

Several techniques are known for the obtains of nanocrystalline materials in the form of thin films or coatings on various conductive or non-conductive substrates: chemical or physical vapour deposition (CVD or PVD), sputtering, thermal spray, electrochemical deposition (ED), electroless deposition (EL), etc. [16, 17]. Electrochemical deposition (ED) is technique that is fully compatible with MEMS technologies. It is a low equipment and product cost, low temperature, easy-controlled deposition technique with high deposition rate and environmentally friendly [18, 19]. This technique is suitable for the synthesis of various metal films used in MEMS with satisfactory performance such as: good adhesion strength to the substrate, controlled residual stresses, satisfactory microhardness, good corrosion, wear and creep resistance, uniformity and compactness of the coating. The possibility of selective etching [20, 21] and removal of the layer and most importantly the ability to synthesize materials with a pre-designed thickness and desired structure. The key to designing a functional coating lies in optimizing and selecting adequate electrodeposition parameters and suitable regimes of electrodeposition [22].

The parameters of electrodeposition determining structural-morphological properties, and hence, mechanical characteristics of metal coatings are: the type of cathode, mixing of electrolyte and applied current regime, temperature, the type and composition of electrolyte and etc [3, 23]. Organic or nonorganic additives are added to electrolyte in purpose of change the film microstructure, topography and improvement the mechanical properties such as higher hardness value [3], brightness [24, 25], ductility, roughness or adhesion manner [23, 26]. Synergistically effect of the additives in the plating solution contributes to obtaining the fine-grained film microstructure and high values of composite hardness and adhesion [27, 28]. The type and intensity of electrolyte mixing are also an important factor influencing the modification of the microstructure of the obtained coatings and its microhardness [3, 29-30].

In this study, morphological, structural and mechanical properties of Cu coatings electrodeposited on different hard substrates (Si and brass) by the applied various current regime (pulsating (PS) and direct (DC)) from two different sulfate electrolytes type (without/with additives) were examined. The effect of substrate properties like hardness and roughness on the mechanical behaviours of

electrodeposited Cu coatings was discussed, also. The composite hardness model of Chicot–Lesage (C–L) was chosen and applied to experimental data in order to analyze the composite systems made [9-12]. The basis of theory of the composite hardness model according to Chicot–Lesage (C–L) is given in [23]. Applying the C–L model, the critical relative indentation depth (RID)_c was determined as universal criteria, which is independent of all examined parameters of the current regime, coating thickness and cathode variation. RID represents the normalized depth of indentation in relation to the thickness of the electrodeposited coating. This RID value separated the area in which the composite hardness of the Cu coating corresponded to its absolute hardness from the area in which application of the C–L model was necessary for a determination of the absolute coating hardness [31].

Experimental

Influence of current regime and coating thickness on Cu/Si performance obtained in PC regime

The copper coatings were electrolytically produced by electrodeposition of Cu on the Si(111) hard substrate. Electrodeposition of copper was performed by the pulsating current (PC) regime from *electrolyte I*: 240 g L⁻¹ CuSO₄·5 H₂O in 60 g L⁻¹ H₂SO₄ at the room temperature in an open cell of a prismatic shape. The Si(111) orientation of (1.0 × 1.0) cm² surface area is used as a cathode, and it was placed in the middle of the cell between two parallel Cu anodes [23, 31]. The parameters of the applied PC regime for electrodeposition of Cu coatings are given in Table 1. The regime of pulsating current (PC) is defined by periodic repetitions of current square wave and pause, and it is presented in reference [23].

Table 1. The parameters of the PC regime used for electrodeposition of copper coatings on the Si(111). j_A – the current density amplitude; j_{av} – the average current density; t_c – deposition pulse; t_p – pause duration; ν – frequency; δ – thickness of coating [23].

No.	t_c / ms	t_p / ms	j_A / mA cm ⁻²	j_{av} / mA cm ⁻²	ν / Hz	δ / μ m
1.	5	5	100	50	100	40
2.	5	7.5	100	40	80	40
3.	5	15	100	25	50	40
4.	5	28.3	100	15	30	40
5.	5	5	120	60	100	40
6.	5	5	140	70	100	40
7.	5	5	100	50	100	20
8.	5	5	100	50	100	60

Influence of substrate type with variation coating thickness on Cu/brass and Cu/Si performance

Basic sulfate electrolyte (*electrolyte I*) was used for electrodeposition Cu coatings with variation of coating thickness: 10, 20, 40 and 60 μ m. For the electrodeposition process, the regime of pulsating current (PC) with the following parameters was applied: $j_A = 100$ mA cm⁻², $t_c = 5$ ms, $t_p = 5$ ms, $j_{av} = 50$ mA cm⁻² and $\nu = 50$ Hz. The deposition was done on two different substrates: on Si and brass foil. Preparation of the substrates were given in reference [32].

Influence of electrolyte type with variation substrate type and coating thickness in DC regime

Electrodeposition of copper was performed by a galvanostatic regime of electrolysis (DC mode) at a current density (j) of 50 mA·cm⁻² from the *electrolyte I* and from an electrolyte with addition of leveling and brightening additives that enable a formation of Cu coatings with mirror bright appearance [25] on brass and Si substrates. The compositions of *electrolyte II* was: 240 g L⁻¹ CuSO₄·5H₂O, 60 g L⁻¹ H₂SO₄, 0.124 g L⁻¹ NaCl, 1 g L⁻¹ PEG 6000 (polyethylene glycol), 0.0015 g L⁻¹ MPSA (3–Mercapto–1–propanesulfonic acid) [25]. The mixing of electrolyte was performed using magnetic stirrer (MS; 100 rpm). The coating thickness were 20 and 40 μ m.

Structural-morphological and mechanical characterization

The morphology of the Cu coatings was examined by scanning electron microscope (SEM) – model JEOL JSM-6610LV. The surface topography was examined using atomic force microscope (AFM, TM Microscopes-Veeco) in the contact mode. The values of the arithmetic average of the absolute (R_a) roughness parameters and histograms were obtained using software Gwyddion [33]. The scan area was $(70 \times 70) \mu\text{m}^2$. The mechanical characteristics of the composite were characterized using Vickers microhardness tester “Leitz Kleinharteprüfer DURIMET P” with loads ranging from 2.942 N down to 0.049 N. The dwell time was 25s. For each load, three indentations were made and the diagonals of the indents were measured by optical microscope (Olympus CX41) connected to the computer [23]. The hardness values of Si(111) and brass substrates have been already determined applying the *PSR* (Proportional Specimen Resistance) model [34] and were 7.42 GPa for Si(111) [23] and 1.41 GPa for the brass B36 [32] substrates. The Chicot–Lesage (C–L) composite hardness model was used for a determination of the absolute hardness of the Cu coatings [9-12].

Result and discussion

Figure 1 shows SEM morphologies of the Cu coatings obtained in PS regime from *electrolyte I* on Si substrate with variation an average current densities. Figure 2 shows the 2D, 3D AFM images and appropriate histograms. The values of R_a roughness parameters and an average height of grains (h_{av}) obtained from AFM images for the same Cu coatings are given in Table 2. The value of the Meyer’s composite index (m) [9-12, 30] was given, too.

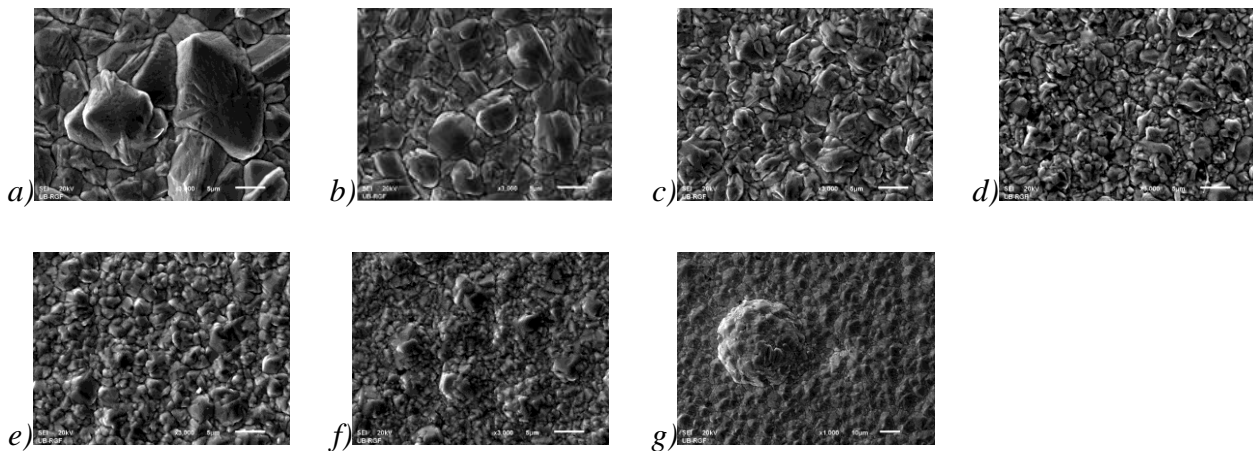


Figure 1. The SEM images of the Cu coatings on Si substrate obtained from *electrolyte I* by the PC regime at j_{av} of: a) 15, b) 25, c) 40, d) 50, e) 60, f) and g) 70 mA cm^{-2} . The thickness of coatings: $\delta = 40 \mu\text{m}$. Microscope magnification are $\times 3000$ and $\times 1000$ (g) [23].

The Cu coating obtained at an average current density of 15 mA cm^{-2} was very coarse, with large and relatively well-defined crystal grains (Figs. 1a and 2a). The coarseness of the coatings decreased with increasing current densities from 15 to 50 mA cm^{-2} . The coatings obtained with 50 and 60 mA cm^{-2} are very similar (Figs. 1d and 1e) and pretty smoother (Figs. 2d, 2e and Table 2). The completely different surface morphology of Cu was obtained at current density at 70 mA cm^{-2} (Figs. 1f, 1g and 2f). This change in surface morphology can be attributed to a decrease of contribution of the activation control and an increase of contribution of the diffusion control with increasing j_{av} value [23]. The formation of globular structures at 70 mA cm^{-2} (Figs. 1f and 1g) is explained by a complete transition to a diffusion-controlled region [23]. This phenomenon can be explained by the increase in the number of smaller grains in relation to large globular structures, so the apparent roughness is lower due to the small number of stochastically distributed globules .

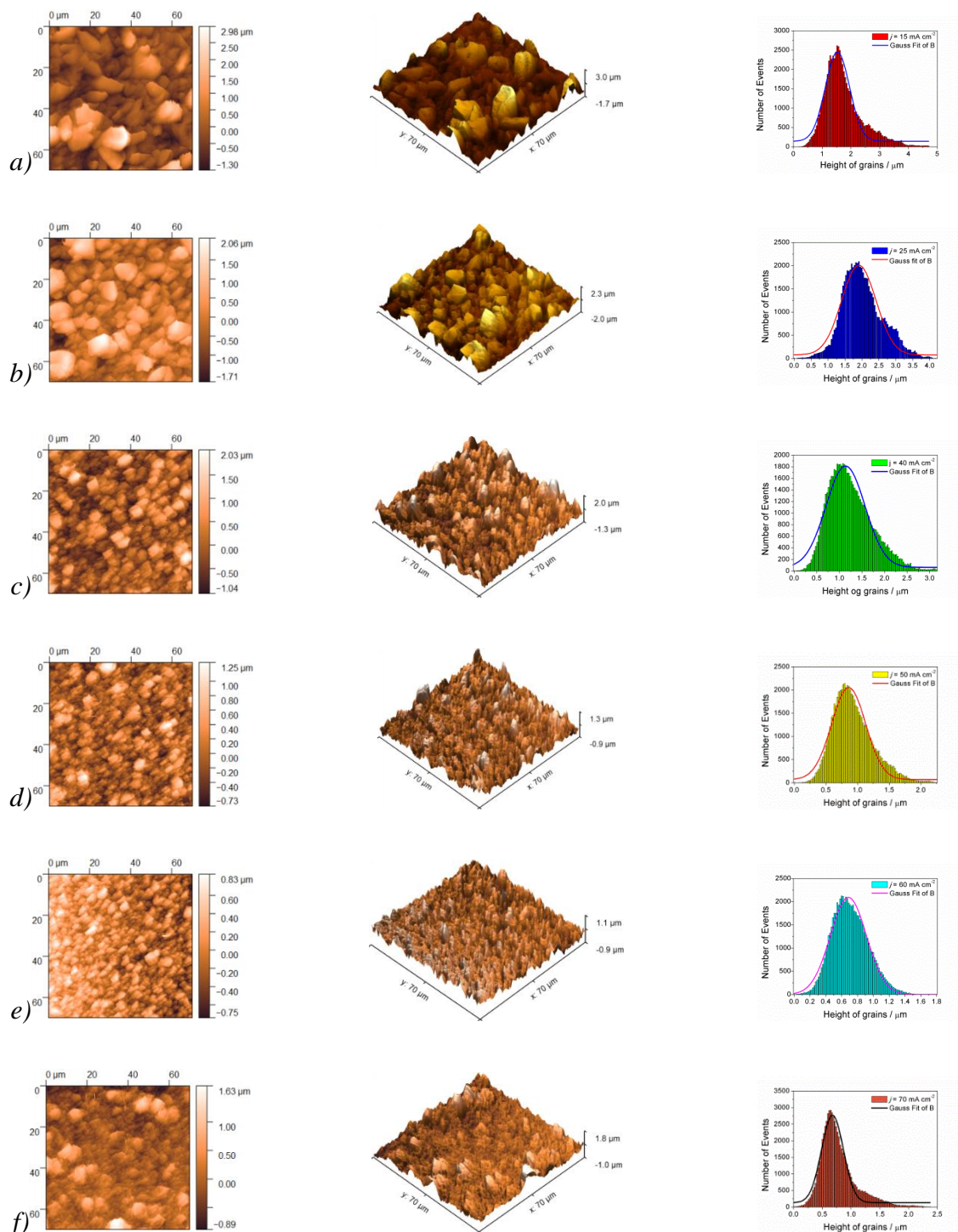


Figure 2. The AFM images and histograms of the Cu coatings on Si substrate obtained from electrolyte I by the PC regime at j_{av} of: a) 15, b) 25, c) 40, d) 50, e) 60, and f) 70 mA cm^{-2} . The thickness of coatings: $\delta = 40 \mu\text{m}$ [23, 31].

Based on the analysis of the surface roughness of Cu coatings, the minimum value of the R_a parameter was obtained in the mixed (activation-diffusion) region (Table 2). However, it is well known that a value of microhardness of coatings strongly depends on its microstructure and coating thickness. For that reason, the Cu coating which had fine-grained structure (Figs 1d and 2d) with minimal roughness, obtained with j_{av} of 50 mA cm^{-2} at 100 Hz, was additionally analyzed by varying its thickness.

Minimal roughness value and an average grain height was obtained for the thinnest coating at 10 μm . With increasing deposition time, i.e. coating thickness in the range of 10-60 μm , the roughness of the sample increased 5.5 times [23]. The optimal parameters established on the Si substrate and same coating thickness were used for deposition on brass, also. The increase of roughness and an average height of grains of the coatings with increasing the thickness are clearly visible from Table 2, and this increase of roughness was about seven times. The change in the topography of the same copper coating can be explained by the influence of the topography of the substrate type. For the 10, 20, 40 and 60 μm thick Cu coatings electrodeposited on the Si(111) substrate, the R_a values of roughness were between 52.42–286 nm and grain height were between 281.3–1092.3. For the Cu coatings of the same thicknesses electrodeposited on the brass, the R_a values were between 75.05–512.03 nm and grain height were between 307.7–1976.7, indicating the increase of the roughness between 50 and 100 % and increase of average grain height between 109 and 180% relative to the Si(111) substrate. This differences can be attributed to different roughness of the brass and the Si(111) substrates. Namely, every surface area which represents cathode, i.e. substrate for electrodeposition process possesses certain roughness [18]. In our case, the roughness of the brass substrate was considerably larger than that for the Si(111) substrate [3].

Table 2. The values of R_a roughness parameters obtained by application of AFM software from (70 \times 70) μm^2 scan area. h_{av} – average height of grains and m – Meyer's index.

$j_{av} / \text{mA cm}^{-2}$	15	25	40	50	60	70
R_a / nm	507.3	470.5	385	169.9	237	229.1
h_{av} / nm	1910	1530	1140	860	685	676
m	0.4288	0.4372	0.4770	0.4979	0.4346	0.3447
<i>Si(111)</i>				<i>Brass B36</i>		
$\delta / \mu\text{m}$	10	20	60	10	20	60
R_a / nm	52.42	101.5	286.3	75.05	146.0	512.03
h_{av} / nm	281.3	459.2	1092.3	307.7	660.2	1976.7
m	0.3257	0.3591	0.4286	0.3082	0.4141	0.3506

Figure 3 shows the dependencies of the composite hardness, H_c , coating hardness, H_{coat} and parameter $(\delta/d)^m$ on the relative indentation depth (RID). RID is defined by a ratio between an indentation depth, h and a thickness of coating, δ as $RID = h/\delta$, where an indentation depth is related with a diagonal size as $h = d/7$ [2, 13, 23, 30-31]. The results of the calculated coating microhardness according to the C–L model more clearly indicate the influence of the current densities change on the microstructure and the hardness of the coating (Figs. 3b and 3e). Assuming that the C–L model is valid up to $(\delta/d)^m = 1$ [12], the limiting or critical RID value of 0.14 $(RID)_c = 0.14$ was determined (Figs. 3c and 3f). It is clear that for RID values larger than 0.14 it is necessary to apply the C–L model in order to determine an absolute hardness of the Cu coatings. On the other hand, for the RID values smaller than this value, the measured composite hardness can be equalled with the coating hardness.

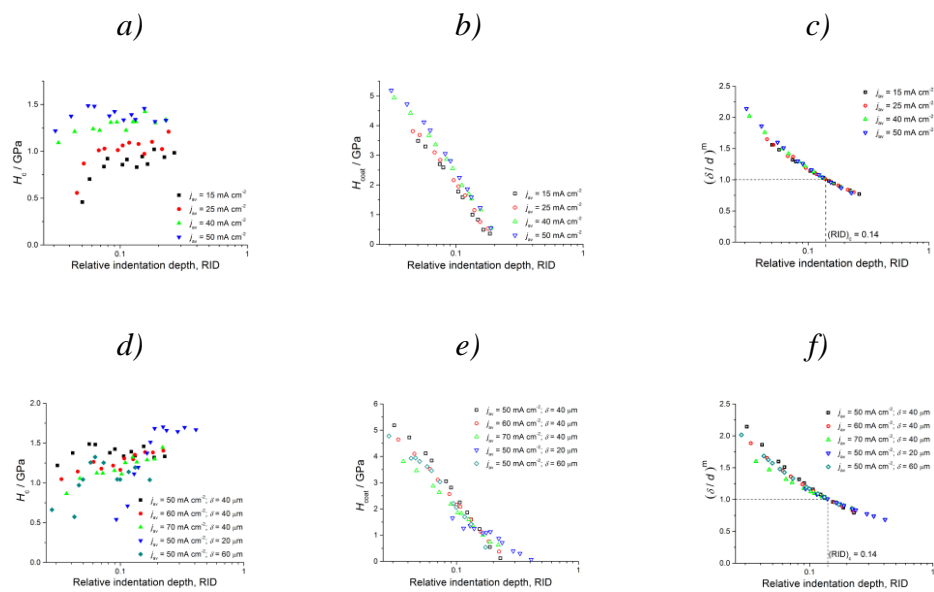


Figure 3. The dependencies of: a) and d) H_c ; b) and e) H_{coat} ; c) and f) $(\delta/d)^m$ values calculated by the C–L model on the RID for the Cu coatings obtained by the PC regime at j_{av} of 15, 25, 40, 50, 60 and 70 mA cm^{-2} for thickness of coatings at 40 μm and for coatings at 20 and 60 μm (d, e, f) [31].

A comparative analysis of the change in microhardness is shown for the Cu/brass composite system (Fig. 4). For the coatings of 10 and 20 μm thickness, the RID values were between 0.1 and 1 indicating a contribution of both the brass and the electrodeposited Cu to the composite hardness (Fig. 4a). With increasing the coating thickness, a contribution of the coating hardness to the composite hardness ($RID < 0.1$) was increased. The similar shape of the dependencies to those obtained for the dependencies of the coating hardness on the RID was observed for coating hardness (Fig. 4b). The largest difference in coating hardness was obtained for the thinner coatings, while the smallest difference was obtained for those which thickness was 60 μm (see Fig. 3e and Fig. 4b). This clearly indicates that the difference in the coatings hardness depth can be attributed to type of used substrate, i.e. various contribution of hardness of the substrate to the determined hardness of the coating [32].

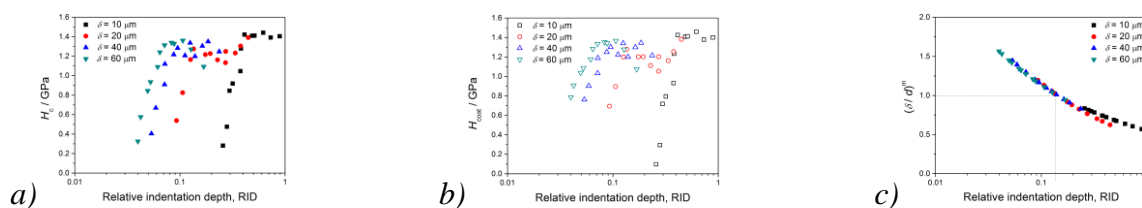


Figure 4. The dependencies of: a) the composite hardness, and b) the coating hardness and d) parameter on the RID for the Cu coatings of the thicknesses of 10, 20, 40 and 60 μm obtained by the PC regime on brass substrate at j_{av} of 50 mA cm^{-2} . The coating hardness and parameters were calculated by application of the Chicot-Lesage (C–L) model [32].

The difference between the Cu coatings (20 μm thick) obtained from the basic electrolyte and from the electrolyte with leveling/brightening additives on the brass in DC/MS regime is given in the Figure 5. The Cu coating obtained from the basic electrolyte was fine-grained with mat appearance and microcrystalline structure (Figure 5a), while the Cu coating obtained from the electrolyte with additives was very smooth without clear boundary among grains, and had mirror bright appearance and nanocrystalline structure (Figure 5b) [3].



Figure 5. The morphology of 20 μm thick Cu coatings on brass substrate obtained by electrodeposition (DC/MS regime) at a current density of 50 mA cm^{-2} on the brass from: (a) electrolyte I, and (b) electrolyte II. Magnification: $\times 1500$ [3].

Figure 6 shows the topography and the corresponding histograms of the coatings obtained without (Figs. 6a, 6c) and with the additives (Figs. 6b, 6d). The roughness of Cu on Si is smaller than for Cu/brass and roughness of 40 μm thick Cu coating obtained from the *electrolyte II* was smaller than that for the 20 μm thick coating time [3]. That can be attributed to good leveling/brightening characteristics of this combination of additives. The X-ray diffraction (XRD) patterns of the Cu coatings obtained without and with additives on Si substrate are shown in [3]. In the Cu coating obtained from the *electrolyte I*, crystallites of Cu were predominately oriented in (220) crystal plane, while in that obtained from the *electrolyte II* were predominately oriented in (200) crystal plane [3].

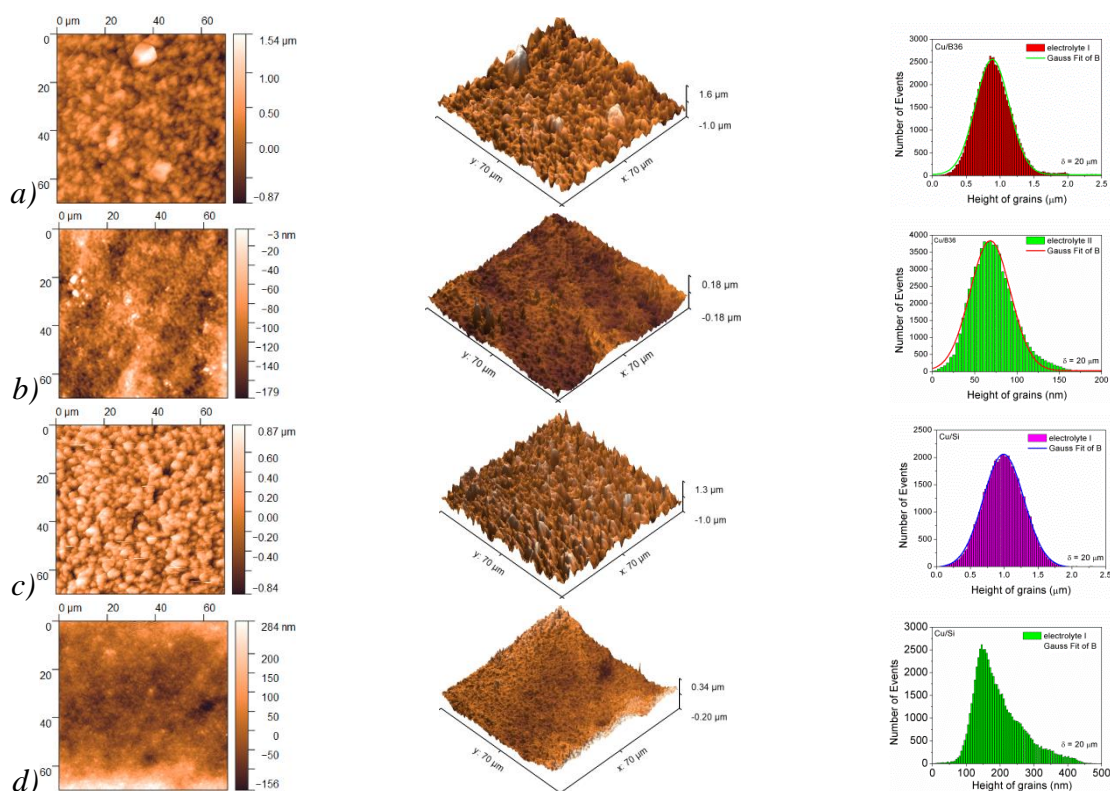


Figure 6. The surface topography and histogram analyses of Cu coatings obtained in DC/MS regime on: a) brass, $\delta = 20 \mu\text{m}$, electrolyte I; b) brass, $\delta = 20 \mu\text{m}$, electrolyte II; c) Si, $\delta = 20 \mu\text{m}$, electrolyte I; d) Si, $\delta = 20 \mu\text{m}$, electrolyte II; Scan size: $(70 \times 70) \mu\text{m}^2$.

The combination of PEG and chloride ions added to acid sulfate electrolyte shows a strong inhibitive effect on the cathodic reaction. On the other hand, MPSA represents top brightening additive and added to the electrolyte acts as an activator of the deposition process [25, 35]. The model of "local perforation" is proposed to explain a synergistic action of these additives in formation of mirror bright Cu coatings [36, 37]. The hardness properties of this samples are shown in reference [3]. The higher coating hardness of Cu coatings obtained from additive free electrolyte can be attributed to numerous

boundaries among grains representing a disruption sites for dislocation motion, or better said, the boundaries among grains prevent a movement of the dislocations [3, 22]. In the case of additives in electrolyte, these boundaries among grains are lost, and dislocation motion has a dominant effect on hardness of these Cu coatings. The hardness value generally increased with decreasing the grain size for mc-coatings and the dislocation pile up mechanism is the basis for a validity of Hall-Petch equation [38]. In case of nc-coatings this mechanism is not applicable because a grain size is less than a certain critical value and then the inverse Hall-Petch equation is valid [39].

Conclusion

It was shown the strong dependence of the microhardness of coatings on their morphology and topography modification for every combination of electrodeposition parameters. The maximal microhardness showed the Cu coating obtained in PS regime on Si at a frequency of 100 Hz with the current density amplitude of 100 mA cm^{-2} and pause duration of 5 ms. The Cu coatings obtained from the basic electrolyte were fine-grained with mat appearance. These coatings showed strong (220) preferred orientation. The smooth mirror bright Cu coatings of strong (200) preferred orientation were obtained from the electrolyte with additives for leveling and brightening. The roughness of the fine-grained coatings was considerably larger than the roughness of smooth coatings. The shapes of the dependencies of the coating hardness calculated by the C–L model on the RID differ mutually for the Cu coatings obtained on the brass and the Si(111) cathodes. This indicated the strong effect of cathode hardness on coating hardness. Applying the C–L model, the limiting value of RID of 0.14 was determined for applied load range. For $\text{RID} > 0.14$, it is necessary to apply the composite hardness model for a determination of absolute or true the coating hardness. For $\text{RID} < 0.14$, the composite hardness corresponds to the coating hardness.

Acknowledgements

This work was funded by Ministry of Education, Science and Technological Development of Republic of Serbia (Grant No. 451-03-68/2022-14/200026).

References

1. M. Schlesinger, M. Paunovic, *Modern electroplating*, New York, Wiley, US, 2011.
2. J. Lamovec, Analysis of the composite and film hardness of electrodeposited nickel coatings on different substrates, *Thin Solid Films*, **516(23)**, 8646–8654, 2008.
3. I.O. Mladenović, Implementation of the Chicot–Lesage Composite Hardness Model in a Determination of Absolute Hardness of Copper Coatings Obtained by the Electrodeposition Processes, *Metals*, **11(11)**, 1807, 2021.
4. E. Broitman, Indentation Hardness Measurements at Macro-, Micro-, and Nanoscale: A Critical Overview, *Tribol. Lett.*, **65(23)**, 1–18, 2017.
5. H. Buckle, *The Science of Hardness Testing and Its Research Applications*, Westbrook, J.W., Conrad, H., Metals Park, Ohio: American Society for Metals, 1973, p. 453.
6. I. Manika, Size effects in micro- and nanoscale indentation, *Acta Mater.*, **54(8)**, 2049–2056.
7. R. Saha, Indentation of a soft metal film on a hard substrate: Strain gradient hardening effects, *J. Mech. Phys. Solids*, **49(9)**, 1997–2014, 2011.
8. A.A. Elmustafa, Indentation size effect in polycrystalline F.C.C. metals. *Acta Mater.*, **50(14)**, 3641–3650, 2002.
9. J. Lesage, New Method to Determine the Hardness of Thin Films, *Rev. Matéria*, **9(1)**, 12–19, 2004.
10. J. Lesage, A model to determine the surface hardness of thin films from standard micro-indentation tests, *Thin Solid Films*, **497(1-2)**, 232–238, 2006.
11. J. Lesage, A model for hardness determination of thin coatings from standard microindentation test, *Surf. Coat. Technol.*, **200(1-4)**, 886–889, 2005.
12. D. Chicot, Absolute hardness of films and coatings, *Thin Solid Films*, **254(1-2)**, 123–130, 1995.

13. A.M. Korsunsky, On the hardness of coated systems, *Surf. Coat. Technol.*, **99(1-2)**, 171–183, 1998.
14. M. Chen, The adhesion of copper films coated on silicon and glass substrates, *Mod. Phys. Lett. B*, **14**, 103–108, 2000.
15. P.J. Burnett, The mechanical properties of wear-resistant coatings. II: Experimental studies and interpretation of hardness, *Thin Solid Films*, **148(1)**, 51–65, 1987.
16. N. Bharadishettar, Coating Technologies for Copper Based Antimicrobial Active Surfaces: A Perspective Review, *Metals*, **11(5)**, 711, 2021.
17. J.F. Rohan, D. Thompson “Frontiers of Cu Electrodeposition and Electroless plating for On-chip Interconnects,” in *Copper Electrodeposition for nanofabrication of Electronics Devices*, K. Kondo, R. N. Alkolkar, D.P. Barkey, M. Yokoi, Ed. New York, Springer, 2014, 99–101.
18. K.I. Popov, S.S. Djokić, N.D. Nikolić, V.D. Jović. Morphology of Electrochemically and Chemically Deposited Metals, Springer International Publishing, New York, 2016.
19. C. Wei, Electrochemical deposition of layered copper thin films based on the diffusion limited aggregation, *Sci. Rep.*, **6**, 34779, 2016.
20. M.S. Ahmad Khair, Sacrificial copper strip sensors for sulfur corrosion detection in transformer oils, *Measurement*, **148**, 106887, 2019.
21. I. Mladenović, Subwavelength nickel-copper multilayers as an alternative plasmonic material, *Opt. Quantum Electron.*, **50(5)**, 203, 2018.
22. I.O. Mladenović, Mechanical features of copper coatings electrodeposited by the pulsating current (PC) regime on Si(111) substrate, *Int. J. Electrochem. Sci.*, **15(11)**, 12173–12191, 2020.
23. I.O. Mladenović, Morphology, Structure and Mechanical properties of copper coatings electrodeposited by pulsating current (PC) regime on Si(111), *Metals*, **10(4)**, 488, 2020.
24. K. Kumar, Effect of thiourea on grain refinement and defect structure of the pulsed electrodeposited nanocrystalline copper, *Surf. Coat. Technol.*, **214**, 8–18, 2013.
25. N.D. Nikolić, Reflection and structural analyses of mirror-bright metal coatings. *J. Solid State Electrochem.*, **8**, 526–531, 2004.
26. L. Magagnin, Adhesion evaluation of immersion plating copper films on silicon by microindentation measurements, *Thin Solid Films*, **434(1)**, 100–105, 2003.
27. I. Mladenovic, Synergetic effect of additives on the hardness and adhesion of thin electrodeposited copper films, *Serb. Jour.El. Eng.*, **14(1)**, 1–11, 2017.
28. L. Bonou, Influence of additives on Cu electrodeposition mechanisms in acid solution: direct current study supported by non-electrochemical measurements. *Electrochim. Acta*, **47(26)**, 4139–4148, 2002.
29. I.O. Mladenović, Influence of intensity of ultrasound on morphology and hardness of copper coatings obtained by electrodeposition, *J. Electrochem. Sci. Eng.*, **12**, 2022.
30. I. Mladenovic, Mechanical characterization of copper coatings electrodeposited onto different substrates with and without ultrasound assistance, *J. Serb. Chem. Soc.*, **84 (7)**, 729–741, 2019.
31. I.O. Mladenović, Determination of the absolute hardness of electrolytically produced copper coatings by application of the Chicot-Lesage composite hardness model, *J. Serb. Chem. Soc.*, OnLine-First (00), 105–105, 2022.
32. I.O. Mladenović, Application of the composite hardness models in the Analysis of Mechanical characteristics of Electrolytically deposited copper coatings: the effect of the type of substrate, *Metals*, **11(1)**, 111, 2021.
33. <http://gwyddion.net/>
34. H. Li, Knoop microhardness anisotropy of single-crystal LaB₆, *Mater. Sci. Eng., A*, **142**, 51–61, 1991.
35. J.J. Kim, Catalytic behavior of 3-mercapto-1-propane sulfonic acid on Cu electrodeposition and its effect on Cu film properties for CMOS device metallization, *J. Electroanal. Chem.*, **542**, 61–66, 2003.
36. W. Plieth, Additives in the electrocrystallization process, *Electrochim. Acta*, **37**, 2115–2121, 1992.
37. L.M. Muresan, S.C. Varvara, Leveling and Brightening Mechanisms in Metal Electrodeposition. In *Metal Electrodeposition*, Nunez, M. Ed.; Nova Science Publishers, Inc., New York, 2005, 1–45.
38. N.J. Petch, The cleavage strength of polycrystals, *J. Iron Steel Inst.*, **174**, 25–28, 1953.
39. A. Varea, Mechanical Properties and Corrosion Behaviour of Nanostructured Cu-rich CuNi Electrodeposited Films, *Int. J. Electrochem. Sci.*, **7**, 1288–1302, 2012.